

# Molecular simulation of liquid–vapor coexistence for NaCl: Full-charge vs scaled-charge interaction models

Cite as: J. Chem. Phys. **153**, 024501 (2020); <https://doi.org/10.1063/5.0012065>

Submitted: 27 April 2020 . Accepted: 19 June 2020 . Published Online: 08 July 2020

 Dina Kussainova,  Anirban Mondal,  Jeffrey M. Young,  Shuwen Yue, and  Athanassios Z. Panagiotopoulos



View Online



Export Citation



CrossMark

## ARTICLES YOU MAY BE INTERESTED IN

[Simulations of activities, solubilities, transport properties, and nucleation rates for aqueous electrolyte solutions](#)

The Journal of Chemical Physics **153**, 010903 (2020); <https://doi.org/10.1063/5.0012102>

[Optimal estimates of self-diffusion coefficients from molecular dynamics simulations](#)

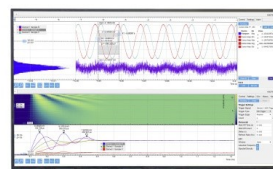
The Journal of Chemical Physics **153**, 024116 (2020); <https://doi.org/10.1063/5.0008312>

[Systematic errors in diffusion coefficients from long-time molecular dynamics simulations at constant pressure](#)

The Journal of Chemical Physics **153**, 021101 (2020); <https://doi.org/10.1063/5.0008316>

Challenge us.

What are your needs for  
periodic signal detection?



Zurich  
Instruments








# Molecular simulation of liquid–vapor coexistence for NaCl: Full-charge vs scaled-charge interaction models

Cite as: *J. Chem. Phys.* **153**, 024501 (2020); doi: [10.1063/5.0012065](https://doi.org/10.1063/5.0012065)

Submitted: 27 April 2020 • Accepted: 19 June 2020 •

Published Online: 8 July 2020



Dina Kussainova,<sup>1</sup>  Anirban Mondal,<sup>2</sup>  Jeffrey M. Young,<sup>2</sup>  Shuwen Yue,<sup>2</sup>   
and Athanassios Z. Panagiotopoulos<sup>2,a)</sup> 

## AFFILIATIONS

<sup>1</sup>Department of Chemical and Materials Engineering, School of Engineering and Digital Sciences, Nazarbayev University, Nur-Sultan, Kazakhstan

<sup>2</sup>Department of Chemical and Biological Engineering, Princeton University, Princeton, New Jersey 08544, USA

<sup>a)</sup>Author to whom correspondence should be addressed: [azp@princeton.edu](mailto:azp@princeton.edu)

## ABSTRACT

Scaled-charge models have been recently introduced for molecular simulations of electrolyte solutions and molten salts to attempt to implicitly represent polarizability. Although these models have been found to accurately predict electrolyte solution dynamic properties, they have not been tested for coexistence properties, such as the vapor pressure of the melt. In this work, we evaluate the vapor pressure of a scaled-charge sodium chloride (NaCl) force field and compare the results against experiments and a non-polarizable full-charge force field. The scaled-charge force field predicts a higher vapor pressure than found in experiments, due to its overprediction of the liquid-phase chemical potential. Reanalyzing the trajectories generated from the scaled-charge model with full charges improves the estimation of the liquid-phase chemical potential but not the vapor pressure.

Published under license by AIP Publishing. <https://doi.org/10.1063/5.0012065>

## I. INTRODUCTION

Molten salts play a number of significant roles in the energy industry. They are used for thermal energy storage,<sup>1,2</sup> as heating and cooling agents in nuclear reactors,<sup>3</sup> and as electrolytes in liquid metal batteries for large-scale grid energy storage.<sup>4,5</sup> Experimental studies of these systems are challenging due to the extreme melting and boiling temperatures of molten salts and their corrosive nature. Molecular simulations can overcome these difficulties and allow access to thermodynamic properties and transport coefficients, given an accurate molecular model.

A commonly used molecular model for alkali halide melts was parameterized by Tosi and Fumi<sup>6</sup> with the Born–Mayer–Huggins–Fumi–Tosi (BMHFT) functional form and full charges (each ion possesses  $\pm 1e$  charge), which has been used in several studies.<sup>7,8</sup> The Michielsen–Woerlee–Graaf (MWG)<sup>9</sup> model was proposed to improve upon BMHFT by incorporating the pressure dependence of compressibility. Both models were developed over 40 years ago and

parameterized to fit only crystal phase properties. In recent years, there have been a significant number of ion models developed that were parameterized on a variety of properties in both liquid and solid phases. However, these models are generally designed to reproduce aqueous solution properties. The most commonly used set of alkali halide ion models was developed by Joung and Cheatham<sup>10</sup> (JC) by fitting to hydration free energies, binding energies, crystal lattice energies, crystal lattice constants, and the ion–water radial distribution functions. While the JC model is part of a class of simple non-polarizable, full-charged, fixed-dipole models, there has been significant focus on the incorporation of polarizability in the last 10 years with implementation in the form of induced dipoles,<sup>11</sup> fluctuating charges,<sup>12</sup> Drude oscillators,<sup>13</sup> and even many-body representations.<sup>14</sup> Many of these implementations drive the computational cost up by significant factors or even an order of magnitude.<sup>15</sup> However, some recently developed force fields have employed scaled charges, which retain the computational efficiency of simple point charge models while implicitly taking into account polarizability.<sup>16</sup>

Alkali halide ion models are generally scaled using the Leontyev–Stuchebrukhov theory to represent a dielectric continuum correction as<sup>17,18</sup>

$$q_{\text{eff}} = \frac{q}{\sqrt{\epsilon_{\text{el}}}}, \quad (1)$$

where  $q_{\text{eff}}$  represents the scaled-charge,  $q$  is the unscaled-charge, and  $\epsilon_{\text{el}}$  represents the high frequency dielectric constant of the medium in which the ions are embedded. Since non-polarizable force fields miss the electronic contribution to the dielectric constant, the charges on the ions are reduced to account for the missing screening effect. Following this method, the groups of Jungwirth,<sup>19–23</sup> Skinner,<sup>24</sup> and Vega<sup>25,26</sup> developed scaled-charge models for many species of alkali halide ions and showed improvements in dynamic and thermodynamic properties of aqueous alkali halide solutions. In fact, scaled-charge models have even been shown to approach the accuracy of polarizable models for dynamic<sup>27</sup> and interfacial properties.<sup>28</sup> Most recently, Zeron *et al.*<sup>26</sup> developed scaled models for a series of monovalent and divalent ions specific for seawater and biological fluids, targeting solution densities, radial distribution functions, hydration number, and adjusted melt/solid densities. They found that while scaled-charge models accurately predicted bulk aqueous properties and water hydration characteristics, molten salt densities were ~20% lower than that of full charge models.

Benavides *et al.*<sup>25</sup> developed an NaCl model, termed here “the Madrid model,” by parameterizing to activity coefficients, liquid and solid densities with concentration dependence, and the difference between solution and crystal free energies. In comparison with a non-polarizable point charge model, the Madrid model achieved closer agreement with experiment for solubility, water activity, mean ionic activity, self-diffusion, and surface tension for concentrations below 2 mol/kg. While it should be acknowledged that the charge scaling introduced for aqueous solutions is not appropriate for molten salts, which typically have a higher density and thus would require higher scaling factors for the charges to represent their effective polarizability, we have chosen to retain the original charge scaling of the Madrid model, since our aim is to investigate the effects of charge scaling on vapor–liquid coexistence properties, rather than develop a new force field for NaCl.

While there have been a number of prior studies on the dynamics, thermodynamics, and interfacial properties of molten salts,<sup>29,30</sup> there are more limited results on the vapor pressure and liquid–vapor coexistence of these systems. Vapor pressure affects the volatility of molten carbonate fuel cells and is critical in the determination of melt losses, which affect electrolyte management and safe operations.<sup>31,32</sup> Guissani and Guillot<sup>7</sup> first obtained coexistence properties for NaCl using the BMHFT model<sup>6</sup> and single-phase molecular dynamics simulations in combination with an analytical equation of state. Rodrigues and Fernandes<sup>8</sup> performed free energy calculations to obtain coexistence properties using both the BMHFT and MWG models for NaCl.<sup>9</sup> There have not been any prior studies of the liquid–vapor coexistence using more recent models that represent a broader set of properties of ionic crystals and aqueous solutions. In particular, the effect of charge scaling on molten salt–vapor coexistence properties remains unknown. While scaled-charge models have been shown to improve dynamic and structural properties of aqueous salt systems, it is unclear how the implicitly represented

polarization translates to liquid–vapor coexistence properties. The calculation of the liquid–vapor coexistence and specifically the vapor pressure serves as a test of the consistency and transferability of the models, highlighting advantages and disadvantages of full-charge and scaled-charge models.

One additional complication that should be acknowledged in connection with the study of the vapor–liquid coexistence is that the two phases have different dielectric environments; charge scaling is appropriate for the bulk liquid, but not for the low-density vapor, for which full charges would be more appropriate. However, as temperature is increased, the two phases become more similar in density and they become identical at the critical point. There is no simple way to represent these changes in a fixed-point-charge model, so we have chosen to keep the model charges the same in the two phases for internal model consistency.

This article is organized as follows. The simulation methods used in this study are presented in Sec. II. Density, chemical potential of liquid NaCl, and liquid–vapor coexistence are presented in Secs. III A–III C, respectively. Finally, Sec. IV provides a summary of the work.

## II. MOLECULAR MODELS AND SIMULATION METHODS

In this work, both non-polarizable full-charge and scaled-charge interaction models are used to represent NaCl. For the full-charge model, the JC<sup>10</sup> interaction parameters are used. For the scaled-charge model, we chose the Madrid model developed by Benavides *et al.*,<sup>25</sup> in which the ion charges are scaled to  $\pm 0.85e$ . The interaction parameters used for our simulations can be found in Tables I and II of the [supplementary material](#).

Classical molecular dynamics (MD) simulations were performed using GROMACS v.2018.<sup>33</sup> The simulations were run for 20 ns with a 2 fs time step using the leap-frog integration method. A cutoff of 0.9 nm was used for both the van der Waals (vdW) and the real-space part of the electrostatic interactions. Standard long-range corrections were considered for vdW interactions, and particle mesh Ewald (PME) summations<sup>34,35</sup> with a Fourier-space grid spacing of 0.1 nm and a sixth-order interpolating function with a relative tolerance of  $1 \times 10^{-6}$  were used for the long-range electrostatic interactions.

For the liquid state simulations, 500 ion pairs of NaCl were simulated in the isothermal–isobaric (*NPT*) ensemble. Finite-size effects in these systems are expected to be minimal due to the screening of electrostatic interactions in ionic melts.<sup>36</sup> Temperature and pressure were set using the Nosé–Hoover thermostat<sup>37,38</sup> and the Parrinello–Rahman barostat<sup>39</sup> with a coupling constant of 1 ps and 2 ps, respectively.

In order to estimate the vapor pressure of the salts, vapor state simulations were performed in the canonical (*NVT*) ensemble with 1 ion pair of NaCl. The canonical velocity rescale thermostat<sup>40</sup> with a 1 ps coupling constant was used to set the temperature of the system.

The liquid–vapor coexistence was calculated using the assumption that the gas phase is an ideal gas of ion pairs. Although this assumption will not be accurate near the critical point, this method should predict a more accurate vapor pressure at low temperature compared to direct coexistence methods. Vapor pressure ( $P_v$ ) is

obtained from the condition of thermodynamic equilibrium at each temperature ( $T$ ), namely, that the chemical potentials ( $\mu$ ) of the liquid and vapor are the same,

$$\mu_{\text{vapor}}(T, P_v) = \mu_{\text{liquid}}(T, P_v). \quad (2)$$

The liquid chemical potential consists of ideal and excess parts,

$$\mu_{\text{liquid}} = \mu_{\text{liquid}}^{\text{id}} + \mu_{\text{liquid}}^{\text{ex}}, \quad (3)$$

where the excess part can be computed from molecular simulations. The ideal part is a function of the temperature and the number of ion pairs ( $N$ ) in the system,

$$\mu_{\text{liquid}}^{\text{id}} = \Delta_f G_{\text{Na}^+}^0 + \Delta_f G_{\text{Cl}^-}^0 + 2RT \ln \frac{NkT}{p^0 V}, \quad (4)$$

where  $P^0 = 1$  bar is the reference state pressure at which the formation free energies ( $\Delta_f G^0$ ) of the ideal gas  $\text{Na}^+$  and  $\text{Cl}^-$  ions are taken from the NIST-JANAF tables at each temperature.<sup>41</sup> It should be noted here that the evaluation of the vapor pressure and the phase envelope do not depend on the values of the formation free energies of  $\text{Na}^+$  and  $\text{Cl}^-$ , only the absolute values of the chemical potentials. Although the liquid–vapor coexistence pressure is unknown, it is expected to be close to zero at low temperatures. In order to avoid iterating in pressure, we assume that the effect of pressure on the liquid chemical potential is small and does not affect the excess part of the chemical potential. If we also assume that the liquid is incompressible, then Eq. (3) can be written as

$$\mu_{\text{liquid}}(T, P_v) = \mu_{\text{liquid}}^{\text{id}}(T, P^*) + \mu_{\text{liquid}}^{\text{ex}}(T, P^*) + \frac{V}{n}(P_v - P^*), \quad (5)$$

where  $P^*$  is the pressure at which the simulation to calculate  $\mu_{\text{liquid}}^{\text{ex}}$  is performed, and  $\frac{V}{n}$  is the partial molar volume. In this work,  $P^*$  was taken to be 1 bar since the coexistence pressure is expected to be very small.

In order to calculate the chemical potential of the vapor, we assumed that the ions form an ideal gas of ion pairs. Under this assumption, the chemical potential is given by

$$\mu_{\text{vapor}}(T, P_v) = \Delta_f G_{\text{NaCl}}^0 + 2RT \ln \frac{P_v}{P^0}, \quad (6)$$

where  $\Delta_f G_{\text{NaCl}}^0$  is the formation free energy of an ideal gas ion pair at the pressure  $P^0$ . Combining Eqs. (5) and (6) into Eq. (2), the vapor pressure at a specific temperature of the system can be calculated by solving for  $P_v$ .

The thermodynamic integration approach by Mester and Panagiotopoulos<sup>42,43</sup> was used to calculate  $\mu_{\text{liquid}}^{\text{ex}}$ . One ion pair was gradually inserted into the melt, and its free energy change was calculated using Bennett's acceptance ratio (BAR)<sup>44</sup> method. Interactions of the inserted ion pair were changed from not interacting to fully interacting with the system by varying first  $\lambda$ , the vdW forces, and then  $\phi$ , the Coulombic interactions, from 0 to 1. For liquid state simulations,  $\lambda$  was equally spaced between 11 values ( $\lambda = [0, 0.1, \dots, 1]$ ), while  $\phi$  was equally spaced between 21 and 18 values for JC and Madrid models, respectively ( $\phi = [0, 0.05, 0.1, \dots, 1]$  for the JC model and  $\phi = [0, 0.05, 0.1, \dots, 0.85]$  for the Madrid model). The total free

energy change of this insertion adds up to the excess chemical potential. The vdW interactions of the inserted ion pair are described by a soft-core Lennard-Jones potential as

$$U_{ij,\text{vdW}} = 4\lambda\epsilon_{ij} \left[ \left( \frac{\sigma_{ij}}{[0.5\sigma_{ij}^6(1-\lambda) + r_{ij}^6]^{1/6}} \right)^{12} - \left( \frac{\sigma_{ij}}{[0.5\sigma_{ij}^6(1-\lambda) + r_{ij}^6]^{1/6}} \right)^6 \right], \quad (7)$$

where  $r_{ij}$  is the distance between species  $i$  and  $j$ , and  $\sigma_{ij}$  and  $\epsilon_{ij}$  are the Lennard-Jones interaction parameters. The Coulombic interaction of the inserted ion pair is described as

$$U_{ij,\text{Coul}} = \frac{\phi q_i q_j}{4\pi\epsilon\epsilon_0 r_{ij}}, \quad (8)$$

where  $q_i$  and  $q_j$  are charges of species  $i$  and  $j$ .

For the vapor chemical potential,  $\Delta_f G_{\text{NaCl}}^0$  is defined as the formation free energy of an ideal gas of NaCl ion pairs at the pressure  $P^0$ ,

$$\Delta_f G_{\text{NaCl}}^0 = \Delta_f G_{\text{Na}^+}^0 + \Delta_f G_{\text{Cl}^-}^0 + G_{\text{NaCl}}^{\text{ig}}(P^0) - G_{\text{Na}^+}^{\text{ig}}(P^0) - G_{\text{Cl}^-}^{\text{ig}}(P^0). \quad (9)$$

Since the vapor simulations were performed at constant volume, we replaced Gibbs free energy (at pressure  $P^0$ ) in Eq. (9) with Helmholtz free energy (at volume  $V^0 = P^0/kT$  for one ion pair), obtaining Eq. (10),

$$\Delta_f G_{\text{NaCl}}^0 = \Delta_f G_{\text{Na}^+}^0 + \Delta_f G_{\text{Cl}^-}^0 + A_{\text{NaCl}}^{\text{ig}}(V^0) - A_{\text{Na}^+}^{\text{ig}}(V^0) - A_{\text{Cl}^-}^{\text{ig}}(V^0) - RT. \quad (10)$$

Periodic boundary conditions with PME electrostatic summations were used, meaning that the calculated free energy must be extrapolated to an infinite simulation box size in order to reach the ideal gas state. BAR was used to find the Helmholtz free energy difference ( $A_{\text{NaCl}}^{\text{ig}}(V^*) - A_{\text{Na}^+}^{\text{ig}}(V^*) - A_{\text{Cl}^-}^{\text{ig}}(V^*)$ ) between a single pair of non-interacting and fully interacting  $\text{Na}^+$  and  $\text{Cl}^-$  ions at different simulation volumes ( $V^*$ ), and the volume was corrected to the desired ideal gas volume of  $V^0 = P^0/kT$  using the dependence of  $A$  on  $V$  for an ideal gas, giving

$$\Delta_f G_{\text{NaCl}}^0 = \Delta_f G_{\text{Na}^+}^0 + \Delta_f G_{\text{Cl}^-}^0 + A_{\text{NaCl}}^{\text{ig}}(V^*) - A_{\text{Na}^+}^{\text{ig}}(V^*) - A_{\text{Cl}^-}^{\text{ig}}(V^*) - RT - RT \ln \left( \frac{V^*}{P^0/kT} \right). \quad (11)$$

Calculations of the vapor–liquid coexistence in the present work are performed with free energy calculations, rather than direct coexistence (interfacial) simulations. The use of either charge scaling or full charges is particularly problematic near interfaces, where the local environment is different from the bulk.

### III. RESULTS AND DISCUSSION

Densities and chemical potentials of liquid NaCl were calculated and validated by comparing with experimental values in different temperature and pressure ranges. Vapor pressures of NaCl

at temperatures of 1200 K, 1500 K, 1800 K, and 2000 K were determined to study the liquid–vapor coexistence.

### A. Density of liquid NaCl

At a pressure of 1 bar, both the JC and Madrid models show a linear decrease of density values with increasing temperature (see Fig. 1) that is in qualitative agreement with experimental measurements by Kirshenbaum *et al.*<sup>45</sup> However, the simulation results underpredict experimental density values by 12% for the JC model and 23% for the Madrid model. Neither model has been parameterized with the molten salt density as a target property. This considerable discrepancy in liquid density has been reported previously for scaled-charge models by Zeron *et al.*<sup>26</sup> and suggests that the size parameters for the ions are not appropriate for the melt phase.

Density for the JC and Madrid models at other pressures can be found in Fig. 1 of the [supplementary material](#). At high pressure and low temperature, density has a linear slope with pressure, suggesting that these values are far away from the critical region. Curvature in the density, indicating an approach to the critical point, can be noticed in the JC model from 0 bar to 1000 bars at 2500 K and for the Madrid model at 2100 K and the same pressures. There are no data at 2500 K for the Madrid model, since the system stops behaving as a liquid above 2100 K and 1 bar, while for the JC model, similar behavior can be observed at 2700 K and 1 bar.

### B. Chemical potential of liquid NaCl

The chemical potential of molten NaCl was calculated using the JC and Madrid models as described in Sec. II. For both cases, the chemical potential linearly increases with increasing temperature, as shown in Fig. 2. Comparisons with experimental values that were taken from the NIST-JANAF tables<sup>41</sup> show that the Madrid model significantly overestimates experimental results by up to 95%, while the JC model overestimates experiments by up to 20%.

The poor performance of the Madrid model in predicting the chemical potential is due to the scaling of the charges. Past simulations of scaled-charge models have found that they consistently

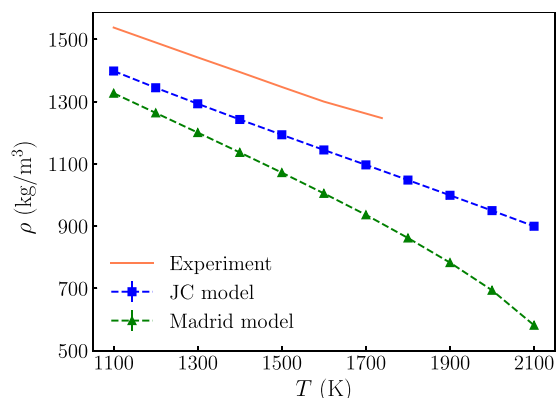


**FIG. 1.** Density of molten NaCl at 1 bar computed using the JC and Madrid models compared to the experimental values by Kirshenbaum *et al.*<sup>45</sup> Standard deviation is less than 0.9 kg/m<sup>3</sup> and 2.3 kg/m<sup>3</sup> for JC and Madrid models, respectively.

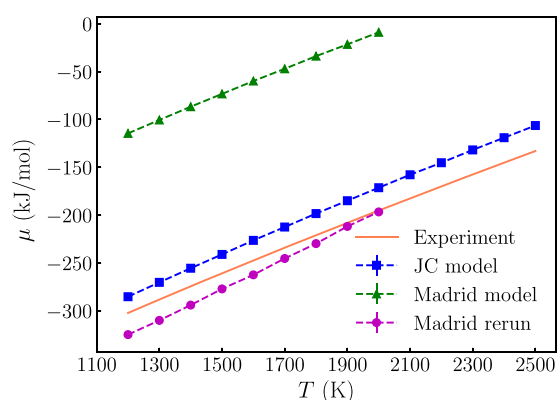


**FIG. 2.** The chemical potential of molten NaCl computed using the JC model, Madrid model, and rerun of the Madrid model with full charges is compared to the experimental values from NIST-JANAF tables.<sup>41</sup> The standard deviations are up to 0.5%, 2.2%, and 1.2% for the JC, Madrid, and Madrid rerun models, respectively.

overestimate the chemical potential since the free energy change of inserting a partial charge is less than that of a full charge.<sup>25,46,47</sup>

However, the scaled-charge models give more realistic interactions between ions, possibly leading to better simulation trajectories. In previous work, Vega<sup>48</sup> suggested that the potential energy surface used to generate configurations should be different than the one used to calculate properties. We applied this idea to the scaled-charge Madrid model by reanalyzing the trajectories generated from the scaled-charge model with full charges. For each step of the insertion, the charges on the inserted ion pair were set from 0 to  $\pm 0.85e$  ( $q = [0, \pm 0.05e, \pm 0.1e, \dots, \pm 0.85e]$ ) for the generation of the trajectory and between 0 and  $\pm 1e$  ( $q = [0, \pm 0.059e, \pm 0.118e, \dots, \pm 1e]$ ) for the calculation of the potential energy in BAR. For this purpose, we used the *rerun* feature in the *gmx mdrun* tool as implemented in Gromacs,<sup>33</sup> and therefore the “Madrid rerun” caption is used to describe the reanalysis of the Madrid model’s trajectories with full charges. As can be seen, new results for the chemical potential of the rerun Madrid model are in close agreement with experimental values, and underestimation is less than 8%. Moreover, chemical potentials at various pressures, starting from 1 bar and ending with 10 000 bars, were calculated for three cases; the results can be found in Fig. 2 of the [supplementary material](#).

### C. Liquid–vapor coexistence of NaCl

To study the vapor phase of NaCl, the system-size effect on the chemical potential results was analyzed first. For this purpose, 1 ion pair of NaCl was simulated in the *NVT* ensemble in different sized boxes ( $L = [2.5 \text{ nm}, 5 \text{ nm}, 7.5 \text{ nm}]$ ). Their chemical potentials were calculated at temperatures 1200 K, 1500 K, 1800 K, and 2000 K and then correlated with the reference state pressure, as described in Sec. II. The standard deviation of the correlated values is up to 1%, as shown in Fig. 3. Since the formation free energy is for the ideal gas state, the effect of the Ewald summation on the calculated value was removed by extrapolating the value of  $\Delta_f G_{\text{NaCl}}^0$  to infinite system size. The effect of the system size on the free energy of inserting an

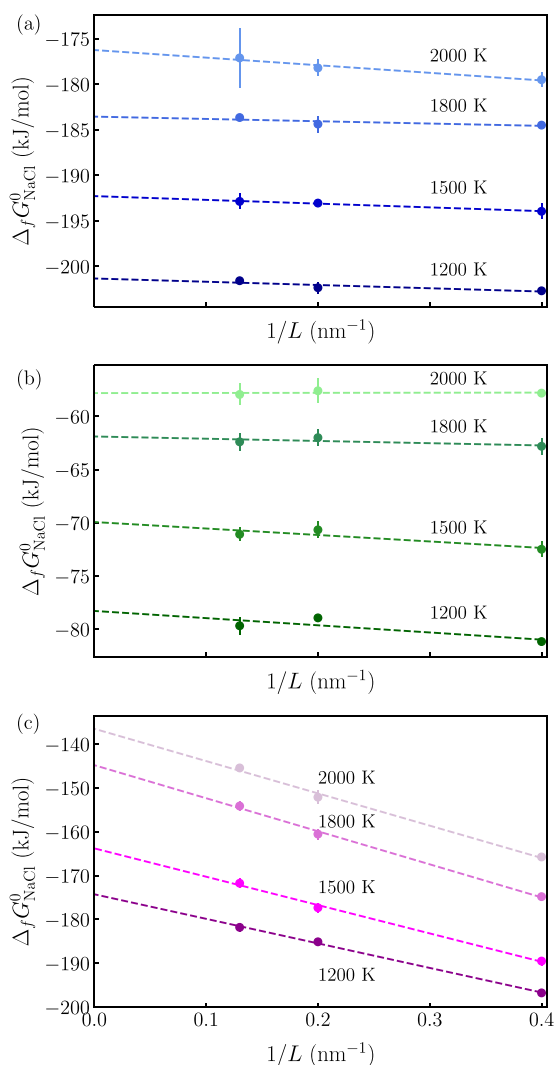


**FIG. 3.** Gibbs free energy of formation correlated with the reference state for (a) JC, (b) Madrid, and (c) rerun of the Madrid model with full charges.

ion pair is expected to be approximately linear with  $1/L$  at infinite dilution.<sup>36,49,50</sup>

Equating liquid and vapor chemical potentials, the vapor pressures at 1200 K, 1500 K, 1800 K, and 2000 K for the JC and Madrid models were calculated and compared to experimental measurements by Stull,<sup>51</sup> as shown in Fig. 4. At high temperatures, the vapor pressures predicted by the Madrid model are close to the experimental ones, while at lower temperatures, the JC model is in closer agreement with experimental values. The results obtained from the rerun of the Madrid model with full charges significantly underpredict the vapor pressure of NaCl. Therefore, even though the liquid chemical potential becomes more accurate when the Madrid model is rerun with full charges, this does not translate to more accurate phase equilibrium properties. All of the models predict a less steep

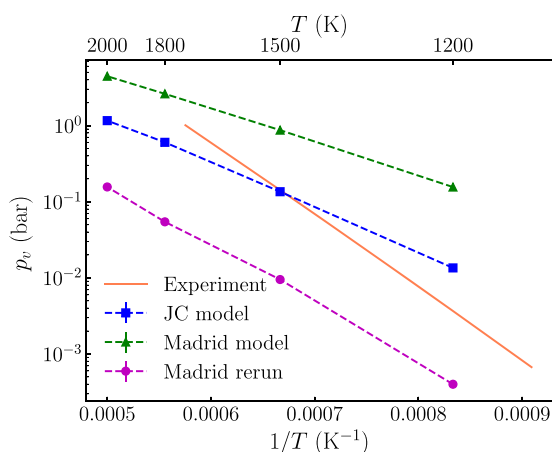


**FIG. 4.** Vapor pressure as a function of temperature for the system with 1 NaCl ion pair is compared to the experimental values by Stull.<sup>51</sup>

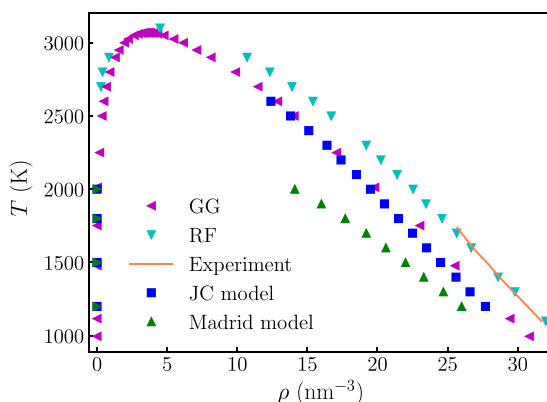


**FIG. 5.** Phase diagram of NaCl computed using JC and Madrid models is compared to the experimental results of Kirshenbaum *et al.*,<sup>45</sup> and simulation results of Guissani and Guillot (GG),<sup>7</sup> and Rodrigues and Fernandes (RF).<sup>8</sup>

slope on Fig. 4 than the experiments, suggesting that the models predict enthalpies of vaporization that are too low.

Furthermore, part of the molten NaCl phase diagram is constructed in Fig. 5 and compared to the experimental measurements of Kirshenbaum *et al.*<sup>45</sup> and simulation results of Guissani and Guillot<sup>7</sup> obtained using the BHMFT model and Rodrigues and Fernandes<sup>8</sup> obtained using the MWG model. While both models underpredict experimental results for the liquid coexistence density, the JC model results are consistent with the BHMFT results of Guissani and Guillot.<sup>7</sup>

#### IV. CONCLUSIONS

Although scaled-charge salt models have shown promising results in predicting properties of electrolyte solutions,<sup>25</sup> it was not known how charge scaling affects the vapor pressure of molten

salts. The chemical potential of a model with scaled-charges has been reported to be systematically higher than the experimental values,<sup>25,46,47</sup> indicating that these models may incorrectly predict phase equilibria. Therefore, the liquid–vapor coexistence of NaCl was studied with non-polarizable full-charge and scaled-charge models. For this purpose, JC interaction parameters with full charges and the Madrid model, which employs charges scaled to  $\pm 0.85e$ , were used.

The vapor pressure of the JC model is of a similar order of magnitude to the experimental values, while the scaled-charge Madrid model was found to have a higher vapor pressure than both experiments and the full charge JC model. This overprediction may be due to the Madrid model predicting too high of a liquid phase chemical potential. Although the interactions between ions may be better represented with scaled charges, when an ion pair is inserted for the calculation of chemical potential, an incomplete charge experiences less attractive interactions than a full charge. As a consequence, the free energy change upon insertion (chemical potential) will be less negative for a scaled-charge potential. To attempt to overcome this issue, we also calculated the chemical potential of the Madrid model by rerunning the scaled-charge trajectories with full charges. Using these rerun trajectories improved the performance of the Madrid model from overestimating the chemical potential by a factor of two to underestimating it by less than 8%. However, the prediction of vapor pressure using these rerun trajectories falls an order of magnitude below experiments and is worse than the vapor pressure calculated for the Madrid model. Another disadvantage of using a rerun trajectory to predict the vapor–liquid equilibrium is that the results will not agree with direct coexistence simulations. Even though the JC model shows better results for vapor pressure than the Madrid model in the temperature range studied, all of the models used in the current work underpredict the experimental enthalpy of vaporization and therefore fail to represent the effect of temperature on vapor pressure. The reason for this may be due to underprediction of ion–ion interactions by the models since both the JC and Madrid models were parameterized for electrolyte solutions.

Although scaled-charge force fields are good for predicting dynamic properties, they fall short in predicting chemical potentials. In order to have a model that can accurately reproduce both ion dynamics as well as vapor–liquid equilibrium, a more explicit representation of polarizability is likely required. However, if dynamic properties are the main objective, scaled-charge models are accurate enough in predicting phase equilibria that they can be used under most conditions.

## SUPPLEMENTARY MATERIAL

The [supplementary material](#) contains tables of interaction parameters for the JC and the Madrid model and plots of the evolution of density and chemical potential of molten NaCl as a function of temperature and pressure.

## ACKNOWLEDGMENTS

Financial support for this work was provided by the Office of Basic Energy Sciences, U.S. Department of Energy, under Award

No. DE-SC0002128. Dina Kussainova thanks the Shakhmardan Yessenov Science and Education Foundation for the Summer Research Scholarship award. Computing resources were provided by the Princeton Institute for Computational Science and Engineering.

## DATA AVAILABILITY

The data that support the findings of this study are available from the corresponding author upon reasonable request.

## REFERENCES

- 1 P. D. Myers and D. Y. Goswami, “Thermal energy storage using chloride salts and their eutectics,” *Appl. Therm. Eng.* **109**, 889–900 (2016).
- 2 M. M. Kenisarin, “High-temperature phase change materials for thermal energy storage,” *Renewable Sustainable Energy Rev.* **14**, 955–970 (2010).
- 3 F. Lantelme and H. Groult, *Molten Salts Chemistry: From Lab to Applications* (Elsevier, 2013).
- 4 H. Kim, D. A. Boysen, J. M. Newhouse, B. L. Spatocco, B. Chung, P. J. Burke, D. J. Bradwell, K. Jiang, A. A. Tomaszowska, K. Wang, W. Wei, L. A. Ortiz, S. A. Barriga, S. M. Poizeau, and D. R. Sadoway, “Liquid metal batteries: Past, present, and future,” *Chem. Rev.* **113**, 2075–2099 (2013).
- 5 D. H. Kelley and T. Weier, “Fluid mechanics of liquid metal batteries,” *Appl. Mech. Rev.* **70**, 020801 (2018).
- 6 M. P. Tosi and F. G. Fumi, “Ionic sizes and born repulsive parameters in the NaCl-type alkali halides—II: The generalized Huggins-Mayer form,” *J. Phys. Chem. Solids* **25**, 45–52 (1964).
- 7 Y. Guissani and B. Guillot, “Coexisting phases and criticality in NaCl by computer simulation,” *J. Chem. Phys.* **101**, 490–509 (1994).
- 8 P. C. R. Rodrigues and F. M. S. Silva Fernandes, “Phase diagrams of alkali halides using two interaction models: A molecular dynamics and free energy study,” *J. Chem. Phys.* **126**, 024503 (2007).
- 9 J. Michielsen, P. Woerlee, F. v. d. Graaf, and J. A. A. Ketelaar, “Pair potential for alkali metal halides with rock salt crystal structure,” *J. Chem. Soc., Faraday Trans. 2* **71**, 1730 (1975).
- 10 I. S. Joung and T. E. Cheatham III, “Determination of alkali and halide monovalent ion parameters for use in explicitly solvated biomolecular simulations,” *J. Phys. Chem. B* **112**, 9020–9041 (2008).
- 11 A. A. Chialvo and P. T. Cummings, “Simple transferable intermolecular potential for the molecular simulation of water over wide ranges of state conditions,” *Fluid Phase Equilib.* **150–151**, 73–81 (1998).
- 12 S. W. Rick, S. J. Stuart, and B. J. Berne, “Dynamical fluctuating charge force fields: Application to liquid water,” *J. Chem. Phys.* **101**, 6141–6156 (1994).
- 13 P. T. Kiss and A. Baranyai, “A new polarizable force field for alkali and halide ions,” *J. Chem. Phys.* **141**, 114501 (2014).
- 14 F. Paesani, P. Bajaj, and M. Riera, “Chemical accuracy in modeling halide ion hydration from many-body representations,” *Adv. Phys.: X* **4**, 1631212 (2019).
- 15 C. Schröder, “Comparing reduced partial charge models with polarizable simulations of ionic liquids,” *Phys. Chem. Chem. Phys.* **14**, 3089–3102 (2012).
- 16 T. G. A. Youngs and C. Hardacre, “Application of static charge transfer within an ionic-liquid force field and its effect on structure and dynamics,” *Chem. Phys. Chem.* **9**, 1548–1558 (2008).
- 17 I. V. Leontyev and A. A. Stuchebrukhov, “Polarizable molecular interactions in condensed phase and their equivalent nonpolarizable models,” *J. Chem. Phys.* **141**, 014103 (2014).
- 18 L. Pegado, O. Marsalek, P. Jungwirth, and E. Wernersson, “Solvation and ion-pairing properties of the aqueous sulfate anion: Explicit versus effective electronic polarization,” *Phys. Chem. Chem. Phys.* **14**, 10248–10257 (2012).
- 19 P. E. Mason, E. Wernersson, and P. Jungwirth, “Accurate description of aqueous carbonate ions: An effective polarization model verified by neutron scattering,” *J. Phys. Chem. B* **116**, 8145–8153 (2012).

- <sup>20</sup>E. Pluhařová, P. E. Mason, and P. Jungwirth, "Ion pairing in aqueous lithium salt solutions with monovalent and divalent counter-anions," *J. Phys. Chem. A* **117**, 11766–11773 (2013).
- <sup>21</sup>M. Kohagen, P. E. Mason, and P. Jungwirth, "Accurate description of calcium solvation in concentrated aqueous solutions," *J. Phys. Chem. B* **118**, 7902–7909 (2014).
- <sup>22</sup>E. Duboué-Dijon, P. E. Mason, H. E. Fischer, and P. Jungwirth, "Hydration and ion pairing in aqueous  $Mg^{2+}$  and  $Zn^{2+}$  solutions: Force-field description aided by neutron scattering experiments and ab initio molecular dynamics simulations," *J. Phys. Chem. B* **122**, 3296–3306 (2018).
- <sup>23</sup>M. Kohagen, P. E. Mason, and P. Jungwirth, "Accounting for electronic polarization effects in aqueous sodium chloride via molecular dynamics aided by neutron scattering," *J. Phys. Chem. B* **120**, 1454–1460 (2016).
- <sup>24</sup>Z. R. Kann and J. L. Skinner, "A scaled-ionic-charge simulation model that reproduces enhanced and suppressed water diffusion in aqueous salt solutions," *J. Chem. Phys.* **141**, 104507 (2014).
- <sup>25</sup>A. L. Benavides, M. A. Portillo, V. C. Chamorro, J. R. Espinosa, J. L. F. Abascal, and C. Vega, "A potential model for sodium chloride solutions based on the TIP4P/2005 water model," *J. Chem. Phys.* **147**, 104501 (2017).
- <sup>26</sup>I. M. Zeron, J. L. F. Abascal, and C. Vega, "A force field of  $Li^+$ ,  $Na^+$ ,  $K^+$ ,  $Mg^{2+}$ ,  $Ca^{2+}$ ,  $Cl^-$ , and  $SO_4^{2-}$  in aqueous solution based on the TIP4P/2005 water model and scaled charges for the ions," *J. Chem. Phys.* **151**, 134504 (2019).
- <sup>27</sup>S. Yue and A. Z. Panagiotopoulos, "Dynamic properties of aqueous electrolyte solutions from non-polarisable, polarisable, and scaled-charge models," *Mol. Phys.* **117**, 3538–3549 (2019).
- <sup>28</sup>J. Škvára and I. Nezbeda, "Surface of aqueous solutions of alkali halides: Layer by layer analysis," *Mol. Simul.* **45**, 358–372 (2018).
- <sup>29</sup>M.-M. Walz and D. van der Spoel, "Molten alkali halides-temperature dependence of structure, dynamics and thermodynamics," *Phys. Chem. Chem. Phys.* **21**, 18516–18524 (2019).
- <sup>30</sup>F. Bresme, M. González-Melchor, and J. Alejandre, "Influence of ion size asymmetry on the properties of ionic liquid-vapour interfaces," *J. Phys.: Condens. Matter* **17**, 3301–3307 (2005).
- <sup>31</sup>H. Mohn and H. Wendt, "Molecular thermodynamics of molten salt evaporation IV. The evaporation of molten carbonates in atmospheres containing  $CO_2$  and water vapour," *Z. Phys. Chem.* **192**, 101–119 (1995).
- <sup>32</sup>S. Frangini and A. Masi, "Molten carbonates for advanced and sustainable energy applications: Part I. Revisiting molten carbonate properties from a sustainable viewpoint," *Int. J. Hydrogen Energy* **41**, 18739–18746 (2016).
- <sup>33</sup>M. J. Abraham, T. Murtola, R. Schulz, S. Páll, J. C. Smith, B. Hess, E. Lindahl, and "Gromacs," "High performance molecular simulations through multi-level parallelism from laptops to supercomputers," *SoftwareX* **1-2**, 19–25 (2015).
- <sup>34</sup>T. Darden, D. York, and L. Pedersen, "Particle mesh Ewald: An  $N \cdot \log(N)$  method for Ewald sums in large systems," *J. Chem. Phys.* **98**, 10089–10092 (1993).
- <sup>35</sup>U. Essmann, L. Perera, M. L. Berkowitz, T. Darden, H. Lee, and L. G. Pedersen, "A smooth particle mesh Ewald method," *J. Chem. Phys.* **103**, 8577–8593 (1995).
- <sup>36</sup>J. M. Young and A. Z. Panagiotopoulos, "System-size dependence of electrolyte activity coefficients in molecular simulations," *J. Phys. Chem. B* **122**, 3330–3338 (2018).
- <sup>37</sup>S. Nosé, "A molecular dynamics method for simulations in the canonical ensemble," *Mol. Phys.* **52**, 255–268 (1984).
- <sup>38</sup>W. G. Hoover, "Canonical dynamics: Equilibrium phase-space distributions," *Phys. Rev. A* **31**, 1695–1697 (1985).
- <sup>39</sup>M. Parrinello and A. Rahman, "Polymorphic transitions in single crystals: A new molecular dynamics method," *J. Appl. Phys.* **52**, 7182–7190 (1981).
- <sup>40</sup>G. Bussi, D. Donadio, and M. Parrinello, "Canonical sampling through velocity rescaling," *J. Chem. Phys.* **126**, 014101 (2007).
- <sup>41</sup>M. W. Chase, *NIST-JANAF Thermochemical Tables*, 4th ed. (American Chemical Society, Washington, DC, 1998).
- <sup>42</sup>Z. Mester and A. Z. Panagiotopoulos, "Temperature-dependent solubilities and mean ionic activity coefficients of alkali halides in water from molecular dynamics simulations," *J. Chem. Phys.* **143**, 044505 (2015).
- <sup>43</sup>Z. Mester and A. Z. Panagiotopoulos, "Mean ionic activity coefficients in aqueous NaCl solutions from molecular dynamics simulations," *J. Chem. Phys.* **142**, 044507 (2015).
- <sup>44</sup>C. H. Bennett, "Efficient estimation of free energy differences from Monte Carlo data," *J. Comput. Phys.* **22**, 245–268 (1976).
- <sup>45</sup>A. D. Kirshenbaum, J. A. Cahill, P. J. McGonigal, and A. V. Grosse, "The density of liquid NaCl and KCl and an estimate of their critical constants together with those of the other alkali halides," *J. Inorg. Nucl. Chem.* **24**, 1287–1296 (1962).
- <sup>46</sup>J. M. Young, C. Tietz, and A. Z. Panagiotopoulos, "Activity coefficients and solubility of  $CaCl_2$  from molecular simulations," *J. Chem. Eng. Data* **65**, 337–348 (2020).
- <sup>47</sup>A. Mondal, J. M. Young, T. A. Barckholtz, G. Kiss, L. Koziol, and A. Z. Panagiotopoulos, "Genetic algorithm driven force field parameterization for molten alkali-metal carbonate and hydroxide salts" *J. Chem. Theory Comput.* (submitted) (2020).
- <sup>48</sup>C. Vega, "Water: One molecule, two surfaces, one mistake," *Mol. Phys.* **113**, 1145–1163 (2015).
- <sup>49</sup>S. Sakane, H. S. Ashbaugh, and R. H. Wood, "Continuum corrections to the polarization and thermodynamic properties of Ewald sum simulations for ions and ion pairs at infinite dilution," *J. Phys. Chem. B* **102**, 5673–5682 (1998).
- <sup>50</sup>P. H. Hünenberger and J. A. McCammon, "Ewald artifacts in computer simulations of ionic solvation and ion-ion interaction: A continuum electrostatics study," *J. Chem. Phys.* **110**, 1856–1872 (1999).
- <sup>51</sup>D. R. Stull, "Vapor pressure of pure substances. Organic and inorganic compounds," *Ind. Eng. Chem.* **39**, 517–540 (1947).